Mice Heterozygous for the Xanthine Oxidoreductase Gene Facilitate Lipid Accumulation in Adipocytes

Noboru Murakami, Toshio Ohtsubo, Yasuo Kansui, Kenichi Goto, Hideko Noguchi, Yoshie Haga, Yusaku Nakabeppu, Kiyoshi Matsumura, Takanari Kitazono

Objective—Xanthine oxidoreductase (XOR) catalyzes the production of uric acid with concomitant generation of reactive oxygen species. XOR has been shown to regulate adipogenesis through the control of peroxisome proliferator–activated receptor γ, but its role in adipose tissue remains unclear. The aim of this study was to examine the role of XOR in adipose tissue using *XOR* genetically modified mice.

Approach and Results—Experiments were performed using 2-, 4-, and 18-month-old XOR heterozygous mice ($XOR^{+/-}$) and their wild-type littermates to evaluate the physiological role of XOR as the mice aged. Stromal vascular fraction cells were prepared from epididymal white adipose tissue in 2-month-old XOR mice to assess adipogenesis. At 18 months, $XOR^{+/-}$ mice had significantly higher body weight, higher systolic blood pressure, and higher incidence of insulin resistance compared with wild-type mice. At 4 months, blood glucose and the expressions of CCAAT enhancer–binding protein β, peroxisome proliferator–activated receptor γ, monocyte chemoattractant protein-1, and tumor necrosis factor α mRNA in epididymal white adipose tissue were significantly higher in $XOR^{+/-}$ than in wild-type mice. Furthermore, histological analysis of epididymal white adipose tissue in $XOR^{+/-}$ mice revealed that adipocyte size and the F4/80-positive macrophage count were increased. Experiments with a high-fat diet exhibited that body weight gain was also significantly higher in $XOR^{+/-}$ than in wild-type mice. In stromal vascular fraction cells derived from $XOR^{+/-}$ mice, the levels of peroxisome proliferator–activated receptor γ, fatty acid–binding protein 4, and CCAAT enhancer–binding protein α mRNA were upregulated, and oxidative stress levels were elevated during differentiation into adipocytes.

Conclusions—These results suggest that the reduction in *XOR* gene expression in mice augments lipid accumulation in adipocytes, accompanied by an increase in oxidative stress, and induces obesity with insulin resistance in older age. (***Arterioscler Thromb Vasc Biol.* 2014;34:44-51.**)

Key Words: adipose tissue ■ obesity ■ xanthine dehydrogenase

Xanthine oxidoreductase (XOR) is a key enzyme in purine catabolism, the process by which purine is converted to xanthine and uric acid.[1] It has been reported that XOR is a critical source of reactive oxygen species (ROS) and nitric oxide and also plays an important role in a variety of physiological[2] and pathophysiological conditions, such as ischemia–reperfusion injury,[3] endothelial dysfunction in diabetes mellitus,[4] and various cardiovascular diseases.[5–9]

Furthermore, XOR is a structural component of membrane-encapsulated milk fat globules,[10] and mice lacking XOR have defects in fat droplet secretion.[11] We also showed that *XOR* gene disruption induced the deletion of uric acid and the accumulation of triglyceride-rich substances and crystals in the renal tubules, with increased expression of adipogenesis-related genes such as peroxisome proliferator–activated receptor (PPAR) γ and the CCAAT enhancer–binding proteins (C/EBP) β and C/EBPα.[12] These findings suggest that XOR may be implicated in lipid metabolism and adipogenesis.

In a study on adipocyte differentiation using 3T3-L1 preadipocytes, it was reported that XOR lies downstream of C/EBPβ and upstream of PPARγ in the signaling pathway responsible for regulating adipocyte differentiation.[13] Furthermore, Hallenborg et al[14] have shown that XOR and epidermal-type lipoxygenase 3 may synergistically activate PPARγ and promote adipocyte differentiation through the activity of ROS produced by XOR. These studies using 3T3-L1 preadipocytes in vitro have suggested the possibility that decreased XOR activity may correlate with a reduction in lipid accumulation. However, the precise role of XOR in adipogenesis in vivo is not fully understood.

In this study, therefore, we used XOR heterozygous ($XOR^{+/-}$) knockout mice to investigate the role of XOR activity in adipogenesis in vivo and also analyzed the effects of aging and intake of a high-fat diet (HFD) on the phenotype of $XOR^{+/-}$ mice. In addition, we examined adipogenesis using adipose tissue–derived stromal vascular fraction (SVF) cells

Received on: May 13, 2013; final version accepted on: October 11, 2013.

From the Department of Medicine and Clinical Science, Graduate School of Medical Sciences (N.M., T.O., Y.K., K.G., H.N., Y.H., K.M., T.K.), Division of Neurofunctional Genomics, Department of Immunobiology and Neuroscience, Medical Institute of Bioregulation (Y.N.), and Research Center for Nucleotide Pool (Y.N.), Kyushu University, Fukuoka, Japan.

The online-only Data Supplement is available with this article at http://atvb.ahajournals.org/lookup/suppl/doi:10.1161/ATVBAHA.113.302214/-/DC1.

Correspondence to Toshio Ohtsubo, MD, PhD, Department of Medicine and Clinical Science, Graduate School of Medical Sciences, Kyushu University, Maidashi 3-1-1, Higashi-ku, Fukuoka 812-8582, Japan. E-mail tohtsubo@intmed2.med.kyushu-u.ac.jp

Arterioscler Thromb Vasc Biol **is available at http://atvb.ahajournals.org** **DOI: 10.1161/ATVBAHA.113.302214**

Nonstandard Abbreviations and Acronyms	
C/EBP	CCAAT enhancer–binding proteins
eWAT	epididymal white adipose tissue
FABP4	fatty acid–binding protein 4
HFD	high-fat diet
MCP-1	monocyte chemoattractant protein-1
Nox4	NADPH oxidase 4
PPAR	peroxisome proliferator–activated receptor
ROS	reactive oxygen species
SVF	stromal vascular fraction
TNF	tumor necrosis factor
XOR	xanthine oxidoreductase
XOR$^{+/-}$	xanthine oxidoreductase heterozygous
WT	wild type

prepared from XOR$^{+/-}$ mice and their wild-type (WT) littermates. The SVF cells are a heterogeneous cell population that includes adipocyte progenitor cells (preadipocytes).[15,16] Furthermore, preadipocytes in the SVF can differentiate into adipocytes by adequate hormonal stimulation. SVF cells, including macrophages and all components of adipose tissue except mature lipid-laden adipocytes, are closer to the physiological conditions of adipose tissue than 3T3-L1 cells. Thus, we used SVF cells prepared from *XOR* gene–disrupted mice to evaluate the role of XOR on adipogenesis in vitro.

Methods

Materials and Methods are available in the online-only Supplement.

Results

Reduction in *XOR* Gene Expression Facilitates an Increase in Body Weight With Aging

XOR$^{+/-}$ mice at 18 months of age showed significant increases in body weight (47.1±1.4 versus 39.4±0.6 g; $P<0.05$), epididymal fat pad weight (2.4±0.2 versus 1.4±0.1 g; $P<0.05$), and liver weight compared with WT mice without alteration of food intake (Figure 1A, 1C, and 1D and Figure I in the online-only Data Supplement). Systolic blood pressure was higher in XOR$^{+/-}$ mice than in WT mice (96.1±0.7 versus 90.7±0.9 mm Hg; $P<0.05$; Figure 1B). XOR$^{+/-}$ mice also showed significant increases in fasting blood glucose (145±4 versus 108±5 mg/dL; $P<0.05$), insulin concentrations (2.2±0.2 versus 1.5±0.2 ng/mL; $P<0.05$), and homeostasis model assessment of insulin resistance (20.4±1.8 versus 10.4±1.7; $P<0.05$) compared with WT mice (Figure 1F–1H), indicating obesity-associated impairment of glucose tolerance. However, the serum concentrations of cholesterol, triglyceride, and free fatty acids were not different between 18-month-old WT and XOR$^{+/-}$ mice (Table I in the online-only Data Supplement). The serum uric acid concentrations of XOR$^{+/-}$ mice were approximately half those of WT mice (Figure 1E). Inflammation of adipose tissue is associated with obesity-related insulin resistance. To assess the inflammation in epididymal white adipose tissue (eWAT), we performed quantitative reverse transcriptase-polymerase chain reaction

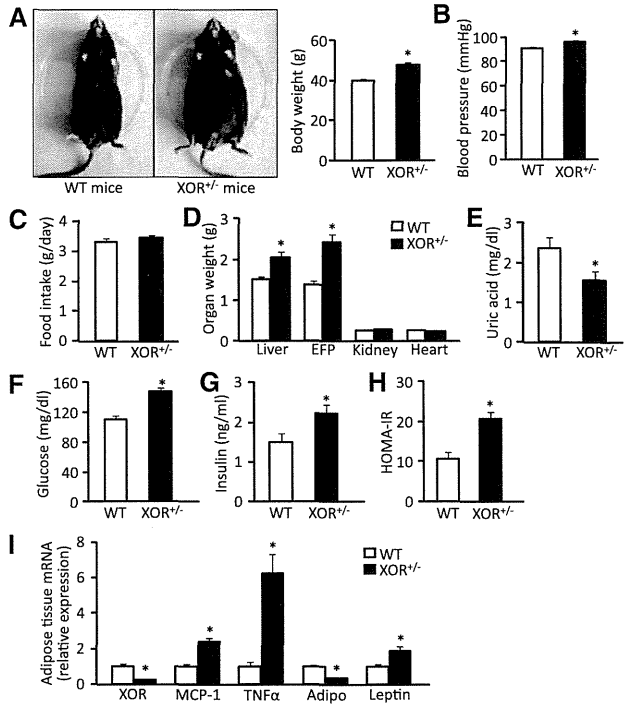

Figure 1. Reduction in xanthine oxidoreductase (*XOR*) gene expression facilitates an increase in body weight with aging. **A** to **C**, Wild-type (WT; n=10) and XOR heterozygous (XOR$^{+/-}$) mice (n=14) at 18 months of age. **A**, Body weights. **B**, Systolic blood pressure. **C**, Daily food intake. **D**, Organ weights. **E–H**, n=10 mice per group. **E**, Serum uric acid concentrations. **F**, Fasting serum glucose levels. **G**, Fasting serum insulin concentrations. **H**, Homeostasis model assessment of insulin resistance (HOMA-IR). Quantitative reverse transcriptase-polymerase chain reaction on epididymal white adipose tissue. **I**, n=8 mice per group. Data are normalized by the expression of TATA-binding protein. *$P<0.05$ compared with WT. Adipo indicates adiponectin; EFP, epididymal fat pad; MCP, monocyte chemoattractant protein; and TNF, tumor necrosis factor.

analysis on the eWAT. XOR$^{+/-}$ mice showed increases in the expression of monocyte chemoattractant protein-1 (MCP-1), tumor necrosis factor (TNF) α, and leptin mRNA and a decrease in the level of adiponectin mRNA, indicating that reduction in XOR expression caused the inflammation in eWAT (Figure 1I). XOR activity in eWAT at 2 and 12 months of age was 10- to 50-fold higher than in other tissues such as liver, kidney, and heart tissue (Figure IIA and IIB in the online-only Data Supplement), which suggested that XOR may play an important role in white adipose tissue.

XOR$^{+/-}$ Mice at 4 Months of Age Exhibit Impaired Glucose Tolerance Without Obesity

Phenotypic analysis of XOR$^{+/-}$ mice at 4 months of age showed that there were no differences in body weight and heart, kidney, and liver tissue weights, but the amount of eWAT was significantly greater in XOR$^{+/-}$ mice than in WT mice (Figure 2A and 2B). The area under the curve of blood glucose concentrations (2.4±0.3 versus 2.0±0.4 [mg/dL]×min×10^4; $P<0.05$) in the intraperitoneal glucose tolerance test, fasting serum insulin (1.4±0.1 versus 1.1±0.1 ng/mL; $P<0.05$), and homeostasis model assessment of insulin resistance (11.5±1.4 versus 7.3±0.6; $P<0.05$) was increased in XOR$^{+/-}$ mice compared

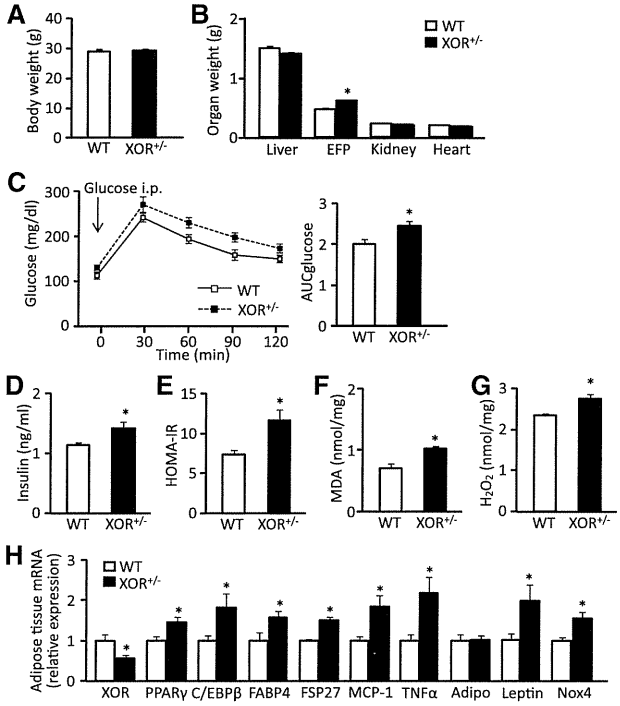

Figure 2. Xanthine oxidoreductase heterozygous (XOR$^{+/-}$) mice at 4 months of age exhibit insulin resistance without obesity. **A** and **B**, Wild-type (WT; n=16) and XOR$^{+/-}$ mice (n=16). **A**, Body weights. **B**, Organ weights. **C**, Intraperitoneal glucose tolerance test, n=10 mice per group. Fasting serum insulin concentrations (**D**) and homeostasis model assessment of insulin resistance (HOMA-IR; **E**), n=8 mice per group. Levels of lipid peroxidation in epididymal white adipose tissue (eWAT) using thiobarbituric acid reactive substances assay (**F**), n=8 mice per group. The release of H_2O_2 from eWAT (**G**), n=12 mice per group. Quantitative reverse transcriptase-polymerase chain reaction on eWAT (**H**), n=8 mice per group. Data are normalized by TATA-binding protein. *P<0.05 compared with WT. Adipo represents adiponectin; AUC, area under the curve; C/EBP, CCAAT enhancer–binding protein; FABP4, fatty acid–binding protein 4; FSP27, fat-specific protein 27; MCP, monocyte chemoattractant protein; Nox4, nicotinamide adenine dinucleotide phosphate oxidase 4; PPAR, peroxisome proliferator–activated receptor; and TNF, tumor necrosis factor.

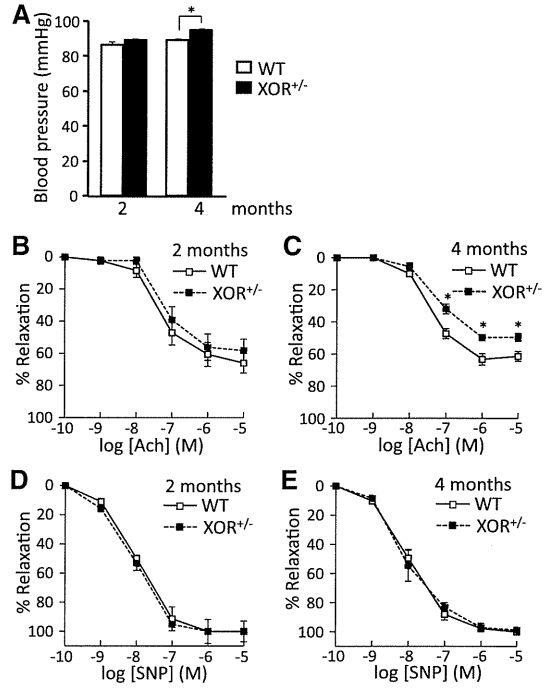

Figure 3. Cardiovascular phenotype of xanthine oxidoreductase heterozygous (XOR$^{+/-}$) mice at 2 and 4 months of age. Systolic blood pressure (**A**), n=10 per group. Vascular endothelium–dependent relaxation at 2 months (**B**) and 4 months (**C**), n=5 per group. Vascular endothelium–independent relaxation at 2 months (**D**) and 4 months (**E**), n=5 per group. *P<0.05 compared with wild type (WT). Ach indicates acetylcholine; and SNP, sodium nitroprusside.

with WT mice (Figure 2C–2E). Systolic blood pressure was increased, and endothelial-dependent relaxation was attenuated in XOR$^{+/-}$ mice compared with WT mice (Figure 3). Serum concentrations of lipids were not different between XOR$^{+/-}$ and WT mice (Table I in the online-only Data Supplement). In addition, the expressions of C/EBPβ, PPARγ, fatty acid–binding protein 4 (FABP4), fat-specific protein 27, leptin, nicotinamide adenine dinucleotide phosphate oxidase 4 (Nox4), MCP-1, and TNFα mRNA were significantly increased in the eWAT of XOR$^{+/-}$ mice (Figure 2H). The oxidative stress level evaluated by the production of malondialdehyde and H_2O_2 in eWAT was also elevated in XOR$^{+/-}$ mice compared with WT mice (Figure 2F and 2G).

To assess the histological change, sections of eWAT were stained with hematoxylin and eosin. Enlarged adipocytes were found in XOR$^{+/-}$ mice compared with WT mice, and the average value of the adipocyte area was significantly greater in XOR$^{+/-}$ mice (3.45±0.04 versus 2.94±0.04 $\mu m^2 \times 10^3$; Figure 4A). Enlargement of the adipocytes releases higher amounts of proinflammatory mediators such as leptin and lower amounts of adiponectin. To quantify macrophage infiltration in the eWAT, immunohistochemical staining using the macrophage-specific marker F4/80 was performed. The percentage of F4/80-positive macrophages in XOR$^{+/-}$ mice was increased 5-fold compared with WT mice. Crown-like structures, which were associated with dead adipocytes surrounded by macrophages, were observed only in the eWAT of XOR$^{+/-}$ mice (Figure 4B).

High-Fat Diet Facilitates an Increase in Body Weight of XOR$^{+/-}$ Mice Compared With WT Mice

To investigate the influence of the XOR genotype on HFD-induced obesity, WT and XOR$^{+/-}$ mice at 2 months of age were fed a normal diet or HFD for 2 or 10 weeks. Body weight gain was similar for the 2 normal diet mouse groups, but between the 2 HFD groups, it was significantly increased in XOR$^{+/-}$ mice compared with the WT mice (45.9±0.7 versus 40.7±0.8 g; P<0.05; Figure 5A) without alteration of food intake (Figure III in the online-only Data Supplement). There were no differences in body or liver weight after 2 weeks with an HFD, but the amount of eWAT was significantly greater in XOR$^{+/-}$ HFD mice than in WT HFD mice (Figure 5B). Glucose tolerance evaluated by intraperitoneal glucose tolerance test was impaired, and fasting serum insulin levels (3.3±0.4 versus 1.8±0.3 ng/mL; P<0.05) and homeostasis model assessment of insulin resistance (31.3±4.7 versus 14.4±3.1; P<0.05) were increased in XOR$^{+/-}$ HFD mice compared with WT HFD mice (Figure 5C–5E). XOR$^{+/-}$ HFD mice showed increases

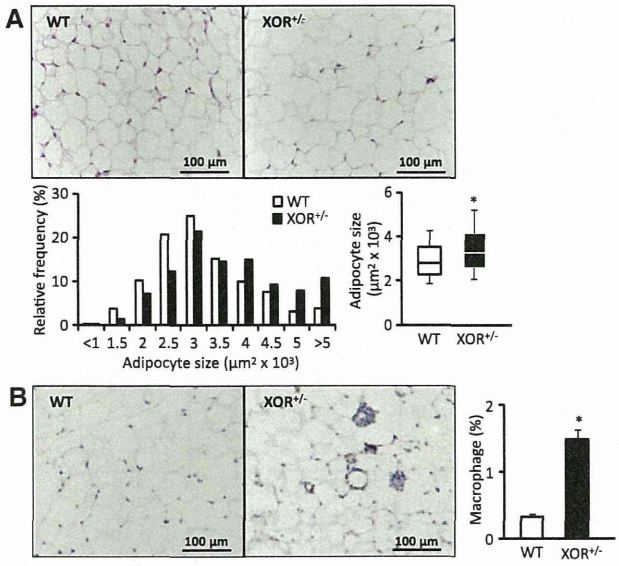

Figure 4. Increased inflammation and oxidative stress in epididymal white adipose tissue (eWAT) of xanthine oxidoreductase heterozygous ($XOR^{+/-}$) mice at 4 months of age. Hematoxylin–eosin staining of eWAT. Adipocyte sizes (area per adipocyte, μm^2) are presented (**A**). Box plots show the median area per adipocyte for groups and the 10th to 90th percentiles, n=8 mice per group. The average value of the adipocyte area was significantly higher in $XOR^{+/-}$ mice (3.45±0.04 vs 2.94±0.04 $\mu m^2 \times 10^3$). Immunohistochemical detection of the macrophage-specific antigen F4/80 in eWAT (**B**), n=4 mice per group. Macrophages were stained brown. The percentage of F4/80-positive macrophages within eWAT was markedly increased in $XOR^{+/-}$ mice (1.46±0.15 vs 0.32±0.05%). *P<0.05 compared with wild-type (WT) mice.

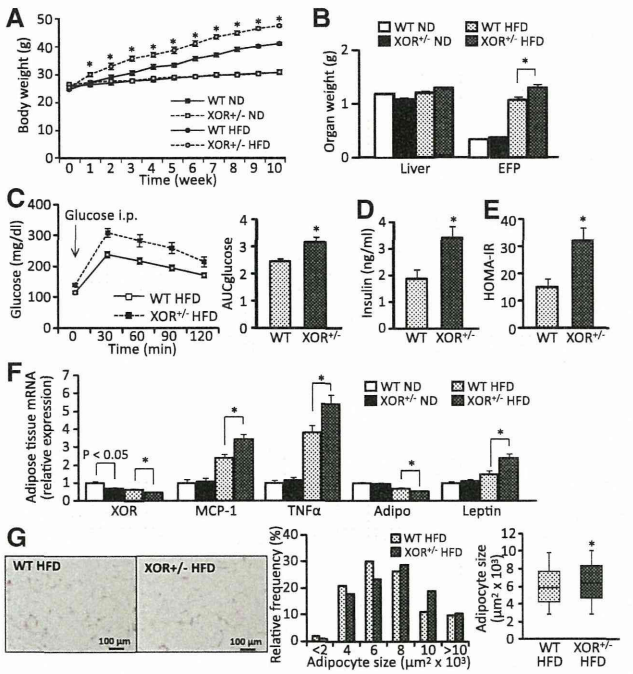

Figure 5. Effects of high-fat diet on xanthine oxidoreductase heterozygous ($XOR^{+/-}$) mice. At 2 months of age, wild-type (WT) and $XOR^{+/-}$ mice were fed a normal diet (ND) or high-fat diet (HFD) for 2 or 10 weeks. Changes in body weight, n=8 mice per group (**A**). **B** to **F** for 2 weeks. **B**, Organ weights, n=8 mice per group. **C** to **G**, n=5 mice per group. **C**, Intraperitoneal glucose tolerance test and area under the curve (AUC) glucose. **D**, Fasting serum insulin concentrations. **E**, Homeostasis model assessment of insulin resistance (HOMA-IR). Quantitative reverse transcriptase-polymerase chain reaction on epididymal white adipose tissue (eWAT; **F**). Data are normalized by the expression of TATA-binding protein (TBP). Hematoxylin–eosin staining of eWAT. Adipocyte sizes (area per adipocyte, μm^2) are presented (**G**). Box plots show the median area per adipocyte for groups and the 10th to 90th percentiles. *P<0.05 compared with WT HFD. Adipo indicates adiponectin; MCP, monocyte chemoattractant protein; and TNF, tumor necrosis factor.

in the expression of MCP-1, TNFα, and leptin mRNA and a decrease in the level of adiponectin mRNA (Figure 5F). In addition, enlarged adipocytes were detected in $XOR^{+/-}$ HFD mice compared with WT HFD mice, and the average value of the adipocyte area was significantly greater in $XOR^{+/-}$ HFD mice (6.51±0.11 versus 6.11±0.11 $\mu m^2 \times 10^3$; P<0.05; Figure 5G). These results suggest that $XOR^{+/-}$ mice facilitate obesity and insulin resistance by upregulation of fat accumulation in mature adipocytes.

SVF Cells Derived From eWAT in $XOR^{+/-}$ Mice Facilitate Adipocyte Differentiation

At 2 months of age, there were no differences in the body weight or eWAT weight between WT and $XOR^{+/-}$ mice. Insulin sensitivity indices, such as the glucose tolerance test, fasting insulin level, and homeostasis model assessment of insulin resistance, in $XOR^{+/-}$ mice were not different from those in WT mice (Figure 6A–6E). Furthermore, the mRNA expressions of the inflammation-related proteins MCP-1 and TNFα in the eWAT were not different between WT and $XOR^{+/-}$ mice, but the mRNA levels of adipocyte differentiation–related proteins such as C/EBPβ, PPARγ, and FABP4 were significantly higher in the eWAT of $XOR^{+/-}$ mice (Figure 6F). The production of H_2O_2 was significantly higher in $XOR^{+/-}$ mice, but the amount of malondialdehyde was not significantly different between the 2 groups (Figure 6G and 6H). We prepared SVF cells from these 2-month-old mice and evaluated their adipocyte differentiation. The SVF cells were differentiated into adipocytes, and accumulated lipids were stained with oil red O on day 7. Lipid accumulation in the differentiated SVF cells was much greater in $XOR^{+/-}$ mice than in WT mice (Figure 7A). The levels of PPARγ, FABP4, and C/EBPα mRNA, which normally increase during adipogenesis, were significantly increased in $XOR^{+/-}$ mice during adipocyte differentiation (Figure 7B). Interestingly, the expression of C/EBPβ mRNA was not induced by the stimulation of adipocyte differentiation, but it was significantly higher in $XOR^{+/-}$ mice than in WT mice during differentiation, suggesting that $XOR^{+/-}$ mice have sustained higher expression levels of C/EBPβ in adipose tissue. The SVF cells derived from $XOR^{+/-}$ mice showed a higher rate of H_2O_2 production compared with those from WT mice during differentiation (Figure 7C). Furthermore, the superoxide level was also significantly increased in $XOR^{+/-}$ mice compared with WT mice by nitroblue tetrazolium reduction assay (Figure 7D). To elucidate the source of ROS production, we examined 3 major pathways of ROS production, namely the XOR-, Nox4- and mitochondria-mediated pathways in the differentiated SVF cells. ROS production in differentiated

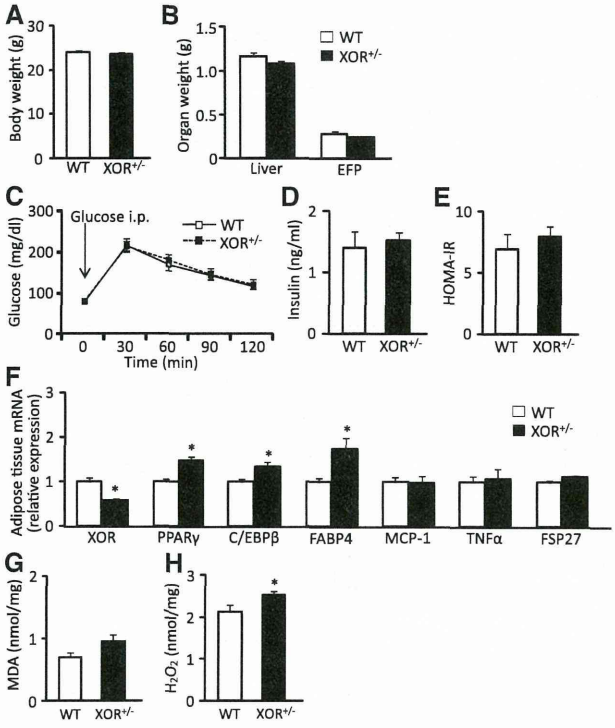

Figure 6. Phenotypic analysis of xanthine oxidoreductase heterozygous ($XOR^{+/-}$) mice at 2 months of age compared with wild-type (WT) mice. **A** to **C**, WT (n=11) and $XOR^{+/-}$ mice (n=11). **A**, Body weights. **B**, Liver and epididymal fat pad weights. **C**, Intraperitoneal glucose tolerance test. **D**, Fasting serum insulin concentrations. **E**, Homeostasis model assessment of insulin resistance (HOMA-IR). Quantitative reverse transcriptase-polymerase chain reaction on epididymal white adipose tissue (eWAT; **F**), n=8 mice per group. Data were normalized by the expression of TATA-binding protein. The release of H_2O_2 from eWAT (**G**), n=10 mice per group. Levels of lipid peroxidation in eWAT using thiobarbituric acid reactive substances assay (**H**), n=10 mice per group. *$P<0.05$ compared with WT mice. C/EBP indicates CCAAT enhancer–binding protein; FABP4, fatty acid–binding protein 4; FSP27, fat-specific protein 27; MDA, malondialdehyde; MCP, monocyte chemoattractant protein; and TNF, tumor necrosis factor.

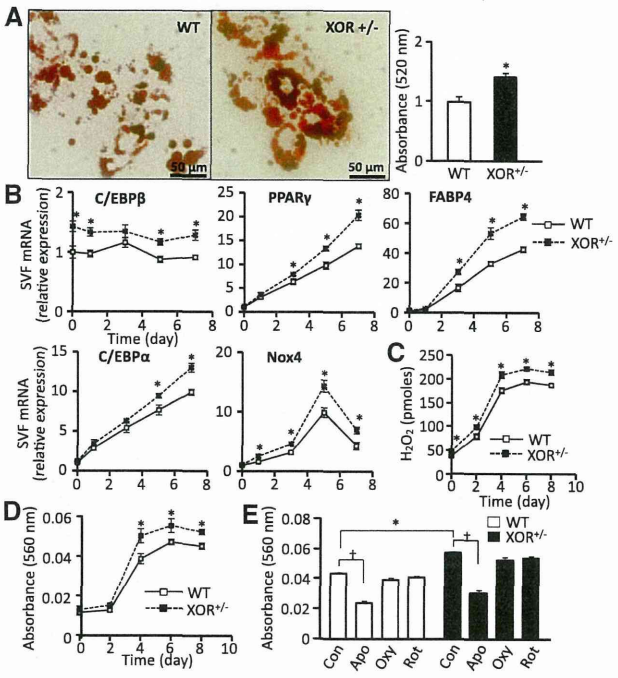

Figure 7. Stromal vascular fraction (SVF) cells derived from epididymal white adipose tissue (eWAT) in xanthine oxidoreductase heterozygous ($XOR^{+/-}$) mice facilitate adipocyte differentiation. Lipid droplets were visualized by oil red O staining at day 7 after differentiation. Quantification of oil red O by measuring 520 nm absorbance (**A**), n=16 per group. Quantitative reverse transcriptase-polymerase chain reaction on SVF cells after differentiation of wild-type (WT) and $XOR^{+/-}$ mice (**B**), n=6 mice per group. Data are normalized by the expression of TATA-binding protein. The release of H_2O_2 from SVF cells during differentiation into adipocytes (**C**), n=8 per group. Reactive oxygen species (ROS) production from SVF cells during differentiation into adipocytes. ROS production was measured by nitroblue tetrazolium reduction, n=8 per group. Dark blue formazan was dissolved, and the absorbance was determined at 560 nm (**D**). Effect of inhibitors of ROS production in SVF cells at day 7 after differentiation. At 1 hour before finishing the incubation, 200 μmol/L apocynin, 100 μmol/L oxypurinol, or 100 μmol/L rotenone was added, and ROS production was measured by nitroblue tetrazolium reduction (**E**). *$P<0.05$ compared with WT. †$P<0.05$ compared with control. Apo indicates apocynin; C/EBP, CCAAT, enhancer-binding protein; Con, control; FABP4, fatty acid–binding protein 4; Nox4, nicotinamide adenine dinucleotide phosphate oxidase 4; Oxy, oxypurinol; PPAR, peroxisome proliferator–activated receptor; and Rot, rotenone.

SVF cells was not suppressed by oxypurinol, an inhibitor of XOR, or by rotenone, an inhibitor of mitochondrial electron transport chain complex I, but was suppressed by apocynin, an inhibitor of nicotinamide adenine dinucleotide phosphate oxidase (Figure 7E). In addition, the expression level of Nox4 mRNA was significantly higher in $XOR^{+/-}$ mice, but the mRNA expression levels of other Nox subunits in $XOR^{+/-}$ mice were not significantly different from those in WT mice (Figure 7B and Figure IV in the online-only Data Supplement). These results suggest that Nox4 is the major source of ROS in differentiated SVF cells and that the SVF cells derived from $XOR^{+/-}$ mice facilitate lipid accumulation in adipocytes exposed to higher oxidative stress during differentiation.

Discussion

In the present study, $XOR^{+/-}$ mice exhibited significantly increased body weight with aging and also showed higher rates of insulin resistance and higher blood pressure levels compared with WT mice. An HFD also induced significant gains in body weight and eWAT weight in $XOR^{+/-}$ mice compared with WT mice. The body weight in $XOR^{+/-}$ mice at 4 months of age was not different from that in WT mice; however, the eWAT in $XOR^{+/-}$ mice exhibited inflammation with macrophage infiltration and accumulated lipids with adipocyte hypertrophy. Furthermore, 4-month-old $XOR^{+/-}$ mice had higher incidence of insulin resistance and higher blood pressure levels compared with WT mice. $XOR^{+/-}$ mice at 2 months of age did not have inflammatory change, insulin resistance, or an increase in blood pressure but had higher expression levels of C/EBPβ, PPARγ, and FABP4 mRNA than in WT mice. In addition, the expression of C/EBPβ mRNA in SVF cells derived from $XOR^{+/-}$ mice was not increased by the stimulation of adipocyte differentiation, but the level of this expression remained higher than in WT mice during differentiation.

These findings suggested that haploinsufficiency of XOR mice might induce sustained higher expression of C/EBPβ, adipocyte differentiation with exaggerated ROS production, and eventually obesity with insulin resistance in older age.

$XOR^{+/-}$ mice at 18 months of age showed obesity with an increase in the expression of MCP-1 mRNA in eWAT. In contrast, the level of adiponectin mRNA was decreased, and oxidative stress levels were upregulated in eWAT. These changes contribute substantially to obesity-related low-grade inflammation in eWAT. The fat accumulation in adipose tissue is associated with not only adipocyte hypertrophy but also an increase in the number of adipocytes. An increase in small adipocytes by adipogenesis usually improves insulin resistance through the production of adiponectin and leptin, whereas hypertrophy of adipocytes exacerbates insulin resistance.[17] TNFα has been observed in the adipose tissue of obese mice with macrophage infiltration[18,19] and has been shown to induce insulin resistance by phosphorylation of the serine residue of insulin receptor substrate-1.[20] It has been reported that ROS production was markedly increased during differentiation of 3T3-L1 preadipocytes into adipocytes and in parallel with fat accumulation in adipocytes.[21] In particular, regulated H_2O_2 production is an essential component of insulin signaling in adipose tissue.[17,22,23] In this study, the SVF cells derived from $XOR^{+/-}$ mice exhibited higher levels of Nox4 expression and H_2O_2 production compared with those in WT mice during differentiation. $XOR^{+/-}$ mice at 4 months of age showed endothelial dysfunction in the aorta and an increase in systolic blood pressure and insulin resistance with no difference in body weight compared with WT mice. These mice had increases in adipose tissue weight, MCP-1, and TNFα mRNA levels and H_2O_2 in eWAT. Histological analysis revealed that eWAT of $XOR^{+/-}$ mice at 4 months of age exhibited a dramatic increase in F4/80-stained macrophage infiltration and an expansion of adipocyte size. These results suggest that the reduction in *XOR* gene expression exaggerated macrophage infiltration, TNFα expression, and H_2O_2 production, resulting in continuous low-grade inflammation and finally obesity with insulin resistance.

Obesity is characterized by increases in the number and size of adipocyte cells and the profound accumulation of triglycerides in adipose tissue. Fat accumulation is induced by an increase in energy intake or a decrease in energy consumption.[24,25] In $XOR^{+/-}$ mice, the amounts of daily food intake and the levels of serum lipids were not different from those in WT mice, but the size of adipocytes was larger and their differentiation was faster than in WT mice. C/EBPβ is induced in the early phase of adipocyte terminal differentiation and lies upstream of PPARγ and C/EBPα in the cascade of adipogenesis. Activation of C/EBPβ induces transcription of both PPARγ and C/EBPα, which in turn coordinately activate metabolic genes such as leptin, FABP4, and adiponectin. In this study, C/EBPβ mRNA in the differentiated SVF cells showed a sustained higher expression in $XOR^{+/-}$ mice than in WT mice from day 0 to day 7, suggesting that a reduction in the *XOR* gene might consistently increase the expression of C/EBPβ mRNA and then induce the cascade of terminal adipocyte differentiation. In fact, there were no differences in body weight or eWAT weight, insulin sensitivity, or inflammation-related mRNA levels between the WT and $XOR^{+/-}$ mice at 2 months of age, but the mRNA expressions of adipocyte differentiation–related proteins, such as C/EBPβ, PPARγ, and FABP4, were significantly increased in $XOR^{+/-}$ mice compared with WT mice.

Recently, Chen et al[26] reported that the amounts of plasma ceramide and spermidine in allopurinol-treated WT mice were the same as those in WT mice, although both compounds were significantly increased in the plasma of $XOR^{-/-}$ and $XOR^{+/-}$ mice. This result suggests that these 2 metabolites were not affected by XOR activity but by *XOR* gene expression. Ceramide and spermidine have been shown to be associated with fat accumulation.[27,28] In addition, it has been reported that ceramide markedly induces the expression of C/EBPβ protein[29] and that spermidine promotes C/EBPβ translation.[30] Although we did not measure the plasma levels of ceramide and spermidine in the present study, these previous findings may support the idea that XOR influences the expression of C/EBPβ and regulates adipocyte differentiation through these metabolites.

The SVF cells derived from $XOR^{+/-}$ mice facilitated fat accumulation with higher oxidative stress. The expressions of PPARγ, FABP4, and C/EBPα mRNA were significantly increased in $XOR^{+/-}$ mice during differentiation. These results explain why the SVF cells prepared from $XOR^{+/-}$ mice showed enhanced adipocyte differentiation. In contrast, previous studies using 3T3-L1 cells or mouse embryonic fibroblasts have shown that the *XOR* gene increased PPARγ activity and adipocyte differentiation.[13,14] It is difficult to account for the conflicting results between the present and previous studies. However, the divergence may be related to the experimental design, that is, previous studies used cells in which *XOR* gene expression was transiently inhibited, but we used haploinsufficient XOR mice that showed chronic inhibition of *XOR* gene expression from birth. These findings may suggest that transient inhibition of the *XOR* gene in 3T3-L1 cells inhibits PPARγ activity and adipocyte differentiation, but chronic inhibition of the *XOR* gene accumulates plasma metabolites, such as ceramide and spermidine, and induces the sustained C/EBPβ expression, oxidative stress, and activation of PPARγ, probably because of an indirect effect of XOR expression in adipose tissue. Furthermore, it has been shown that the adipogenesis of adipogenic cell lines depends on an interplay among adipocyte precursors, vascular cells, and stromal cells.[31] In addition, 3T3-L1 cells express the adipocyte-secreted factor leptin at much lower levels than primary adipocytes. White adipocytes comprise a single large droplet, but 3T3-L1 cells store triglycerides in many droplets.[32] These results suggest that mouse cell lines may not reflect true adipocyte differentiation and real lipid metabolism in vivo.

XOR is a structural component of membrane-encapsulated milk fat globules and is necessary for milk fat droplet envelopment and secretion.[10] The proteins belonging to the cell death–inducing DFF45-like effector family have been shown to associate with lipid droplets. Recently, Wang et al[33] reported that Cidea, a cell death–inducing DFF45-like

effector family protein, is expressed at high levels in lactating mammary glands, induces XOR expression by facilitating the association of C/EBPβ with the promoter of the *XDH* gene, and enhances lipid secretion in vivo. Furthermore, the fat-specific protein 27 (also called Cidec), another cell death–inducing DFF45-like effector family protein, interacts with C/EBPβ to regulate the expression of XOR in adipocytes.[33] In this study, the expression levels of both C/EBPβ and fat-specific protein 27 mRNA in eWAT were significantly higher in 4-month-old $XOR^{+/-}$ mice than in WT mice of the same age. Different fat secretion mechanisms are at work in mammary epithelial cells and adipocytes; however, both the previous and present findings may indicate that XOR plays a pivotal role in adipocytes to regulate fat accumulation.

In conclusion, a reduction in *XOR* gene expression in mice induced fat accumulation and led to obesity with aging through increases in ROS, macrophage infiltration, and insulin resistance. Our study demonstrates that one of the roles of the *XOR* gene may regulate fat metabolism via C/EBPβ expression.

Acknowledgments

We appreciate the technical support from the Research Support Center, Graduate School of Medical Sciences, Kyushu University.

Sources of Funding

This work was supported, in part, by JSPS KAKENHI grant no. 23591195.

Disclosures

None.

References

1. Harrison R. Structure and function of xanthine oxidoreductase: where are we now? *Free Radic Biol Med.* 2002;33:774–797.
2. Ohtsubo T, Rovira II, Starost MF, Liu C, Finkel T. Xanthine oxidoreductase is an endogenous regulator of cyclooxygenase-2. *Circ Res.* 2004;95:1118–1124.
3. Granger DN, Rutili G, McCord JM. Superoxide radicals in feline intestinal ischemia. *Gastroenterology.* 1981;81:22–29.
4. Desco MC, Asensi M, Márquez R, Martínez-Valls J, Vento M, Pallardó FV, Sastre J, Viña J. Xanthine oxidase is involved in free radical production in type 1 diabetes: protection by allopurinol. *Diabetes.* 2002;51:1118–1124.
5. Doehner W, Rauchhaus M, Florea VG, Sharma R, Bolger AP, Davos CH, Coats AJ, Anker SD. Uric acid in cachectic and noncachectic patients with chronic heart failure: relationship to leg vascular resistance. *Am Heart J.* 2001;141:792–799.
6. Amado LC, Saliaris AP, Raju SV, Lehrke S, St John M, Xie J, Stewart G, Fitton T, Minhas KM, Brawn J, Hare JM. Xanthine oxidase inhibition ameliorates cardiovascular dysfunction in dogs with pacing-induced heart failure. *J Mol Cell Cardiol.* 2005;39:531–536.
7. Landmesser U, Spiekermann S, Dikalov S, Tatge H, Wilke R, Kohler C, Harrison DG, Hornig B, Drexler H. Vascular oxidative stress and endothelial dysfunction in patients with chronic heart failure: role of xanthine-oxidase and extracellular superoxide dismutase. *Circulation.* 2002;106:3073–3078.
8. Alef MJ, Vallabhaneni R, Carchman E, Morris SM Jr, Shiva S, Wang Y, Kelley EE, Tarpey MM, Gladwin MT, Tzeng E, Zuckerbraun BS. Nitrite-generated NO circumvents dysregulated arginine/NOS signaling to protect against intimal hyperplasia in Sprague-Dawley rats. *J Clin Invest.* 2011;121:1646–1656.
9. Zuckerbraun BS, Shiva S, Ifedigbo E, Mathier MA, Mollen KP, Rao J, Bauer PM, Choi JJ, Curtis E, Choi AM, Gladwin MT. Nitrite potently inhibits hypoxic and inflammatory pulmonary arterial hypertension and smooth muscle proliferation via xanthine oxidoreductase-dependent nitric oxide generation. *Circulation.* 2010;121:98–109.
10. McManaman JL, Palmer CA, Wright RM, Neville MC. Functional regulation of xanthine oxidoreductase expression and localization in the mouse mammary gland: evidence of a role in lipid secretion. *J Physiol.* 2002;545(Pt 2):567–579.
11. Vorbach C, Scriven A, Capecchi MR. The housekeeping gene xanthine oxidoreductase is necessary for milk fat droplet enveloping and secretion: gene sharing in the lactating mammary gland. *Genes Dev.* 2002;16:3223–3235.
12. Ohtsubo T, Matsumura K, Sakagami K, Fujii K, Tsuruya K, Noguchi H, Rovira II, Finkel T, Iida M. Xanthine oxidoreductase depletion induces renal interstitial fibrosis through aberrant lipid and purine accumulation in renal tubules. *Hypertension.* 2009;54:868–876.
13. Cheung KJ, Tzameli I, Pissios P, Rovira I, Gavrilova O, Ohtsubo T, Chen Z, Finkel T, Flier JS, Friedman JM. Xanthine oxidoreductase is a regulator of adipogenesis and PPARgamma activity. *Cell Metab.* 2007;5:115–128.
14. Hallenborg P, Jørgensen C, Petersen RK, Feddersen S, Araujo P, Markt P, Langer T, Furstenberger G, Krieg P, Koppen A, Kalkhoven E, Madsen L, Kristiansen K. Epidermis-type lipoxygenase 3 regulates adipocyte differentiation and peroxisome proliferator-activated receptor gamma activity. *Mol Cell Biol.* 2010;30:4077–4091.
15. Gimble JM, Bunnell BA, Chiu ES, Guilak F. Concise review: adipose-derived stromal vascular fraction cells and stem cells: let's not get lost in translation. *Stem Cells.* 2011;29:749–754.
16. Madonna R, Geng YJ, De Caterina R. Adipose tissue-derived stem cells: characterization and potential for cardiovascular repair. *Arterioscler Thromb Vasc Biol.* 2009;29:1723–1729.
17. Okuno A, Tamemoto H, Tobe K, Ueki K, Mori Y, Iwamoto K, Umesono K, Akanuma Y, Fujiwara T, Horikoshi H, Yazaki Y, Kadowaki T. Troglitazone increases the number of small adipocytes without the change of white adipose tissue mass in obese Zucker rats. *J Clin Invest.* 1998;101:1354–1361.
18. Xu H, Barnes GT, Yang Q, Tan G, Yang D, Chou CJ, Sole J, Nichols A, Ross JS, Tartaglia LA, Chen H. Chronic inflammation in fat plays a crucial role in the development of obesity-related insulin resistance. *J Clin Invest.* 2003;112:1821–1830.
19. Weisberg SP, McCann D, Desai M, Rosenbaum M, Leibel RL, Ferrante AW Jr. Obesity is associated with macrophage accumulation in adipose tissue. *J Clin Invest.* 2003;112:1796–1808.
20. Rui L, Aguirre V, Kim JK, Shulman GI, Lee A, Corbould A, Dunaif A, White MF. Insulin/IGF-1 and TNF-alpha stimulate phosphorylation of IRS-1 at inhibitory Ser307 via distinct pathways. *J Clin Invest.* 2001;107:181–189.
21. Furukawa S, Fujita T, Shimabukuro M, Iwaki M, Yamada Y, Nakajima Y, Nakayama O, Makishima M, Matsuda M, Shimomura I. Increased oxidative stress in obesity and its impact on metabolic syndrome. *J Clin Invest.* 2004;114:1752–1761.
22. Krieger-Brauer HI, Kather H. Human fat cells possess a plasma membrane-bound H2O2-generating system that is activated by insulin via a mechanism bypassing the receptor kinase. *J Clin Invest.* 1992;89:1006–1013.
23. Mahadev K, Wu X, Zilbering A, Zhu L, Lawrence JT, Goldstein BJ. Hydrogen peroxide generated during cellular insulin stimulation is integral to activation of the distal insulin signaling cascade in 3T3-L1 adipocytes. *J Biol Chem.* 2001:276;21983–21942.
24. Sun K, Kusminski CM, Scherer PE. Adipose tissue remodeling and obesity. *J Clin Invest.* 2011;121:2094–2101.
25. Bleich S, Cutler D, Murray C, Adams A. Why is the developed world obese? *Annu Rev Public Health.* 2008;29:273–295.
26. Chen Q, Park HC, Goligorsky MS, Chander P, Fischer SM, Gross SS. Untargeted plasma metabolite profiling reveals the broad systemic consequences of xanthine oxidoreductase inactivation in mice. *PLoS One.* 2012;7:e37149.
27. van Eijk M, Aten J, Bijl N, Ottenhoff R, van Roomen CP, Dubbelhuis PF, Seeman I, Ghauharali-van der Vlugt K, Overkleeft HS, Arbeeny C, Groen AK, Aerts JM. Reducing glycosphingolipid content in adipose tissue of obese mice restores insulin sensitivity, adipogenesis and reduces inflammation. *PLoS One.* 2009;4:e4723.
28. Jell J, Merali S, Hensen ML, Mazurchuk R, Spernyak JA, Diegelman P, Kisiel ND, Barrero C, Deeb KK, Alhonen L, Patel MS, Porter CW. Genetically altered expression of spermidine/spermine N1-acetyltransferase affects fat metabolism in mice via acetyl-CoA. *J Biol Chem.* 2007;282:8404–8413.
29. Arai N, Masuzaki H, Tanaka T, et al. Ceramide and adenosine 5'-monophosphate-activated protein kinase are two novel regulators of

11beta-hydroxysteroid dehydrogenase type 1 expression and activity in cultured preadipocytes. *Endocrinology*. 2007;148:5268–5277.
30. Hyvönen MT, Koponen T, Weisell J, Pietilä M, Khomutov AR, Vepsäläinen J, Alhonen L, Keinänen TA. Spermidine promotes adipogenesis of 3T3-L1 cells by preventing interaction of ANP32 with HuR and PP2A. *Biochem J*. 2013;453:467–474.
31. Nishimura S, Manabe I, Nagasaki M, Hosoya Y, Yamashita H, Fujita H, Ohsugi M, Tobe K, Kadowaki T, Nagai R, Sugiura S. Adipogenesis in obesity requires close interplay between differentiating adipocytes, stromal cells, and blood vessels. *Diabetes*. 2007;56:1517–1526.
32. Cristancho AG, Lazar MA. Forming functional fat: a growing understanding of adipocyte differentiation. *Nat Rev Mol Cell Biol*. 2011;12:722–734.
33. Wang W, Lv N, Zhang S, Shui G, Qian H, Zhang J, Chen Y, Ye J, Xie Y, Shen Y, Wenk MR, Li P. Cidea is an essential transcriptional coactivator regulating mammary gland secretion of milk lipids. *Nat Med*. 2012;18:235–243.

Significance

Obesity is characterized by increases in the number and size of adipocyte cells and the profound accumulation of triglycerides in adipose tissue. Xanthine oxidoreductase (XOR) is an enzyme that catalyzes the final 2 steps in purine catabolism by converting hypoxanthine to xanthine and xanthine to uric acid, with concomitant generation of reactive oxygen species. In this study, XOR heterozygous ($XOR^{+/-}$) mice showed enhanced lipid accumulation in adipocytes accompanied by an increase in oxidative stress, systolic blood pressure, insulin resistance, and the development of obesity in older age or with high-fat diet. Stromal vascular cells derived from $XOR^{+/-}$ mice differentiated into adipocytes with higher expression levels of peroxisome proliferator–activated receptor γ, fatty acid–binding protein 4, and CCAAT enhancer–binding protein α mRNA compared with $XOR^{+/+}$ mice. The expression of CCAAT enhancer–binding protein β mRNA in $XOR^{+/-}$ mice was sustained at a higher level compared with $XOR^{+/+}$ mice during adipocyte differentiation. $XOR^{+/-}$ mice provide a unique opportunity to study metabolic syndrome.

Supplemental Material

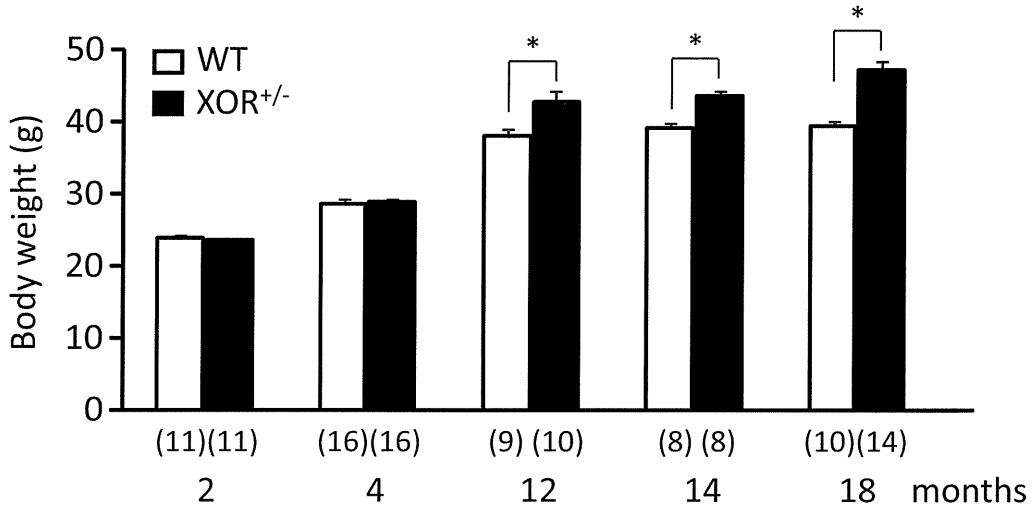

Supplemental Figure I. Body weights of $XOR^{+/-}$ mice at 2, 4, 12, 14 and 18 months of age compared with WT mice. Number of mice was showed in parenthesis. $^{*}P < 0.05$ compared with WT mice.

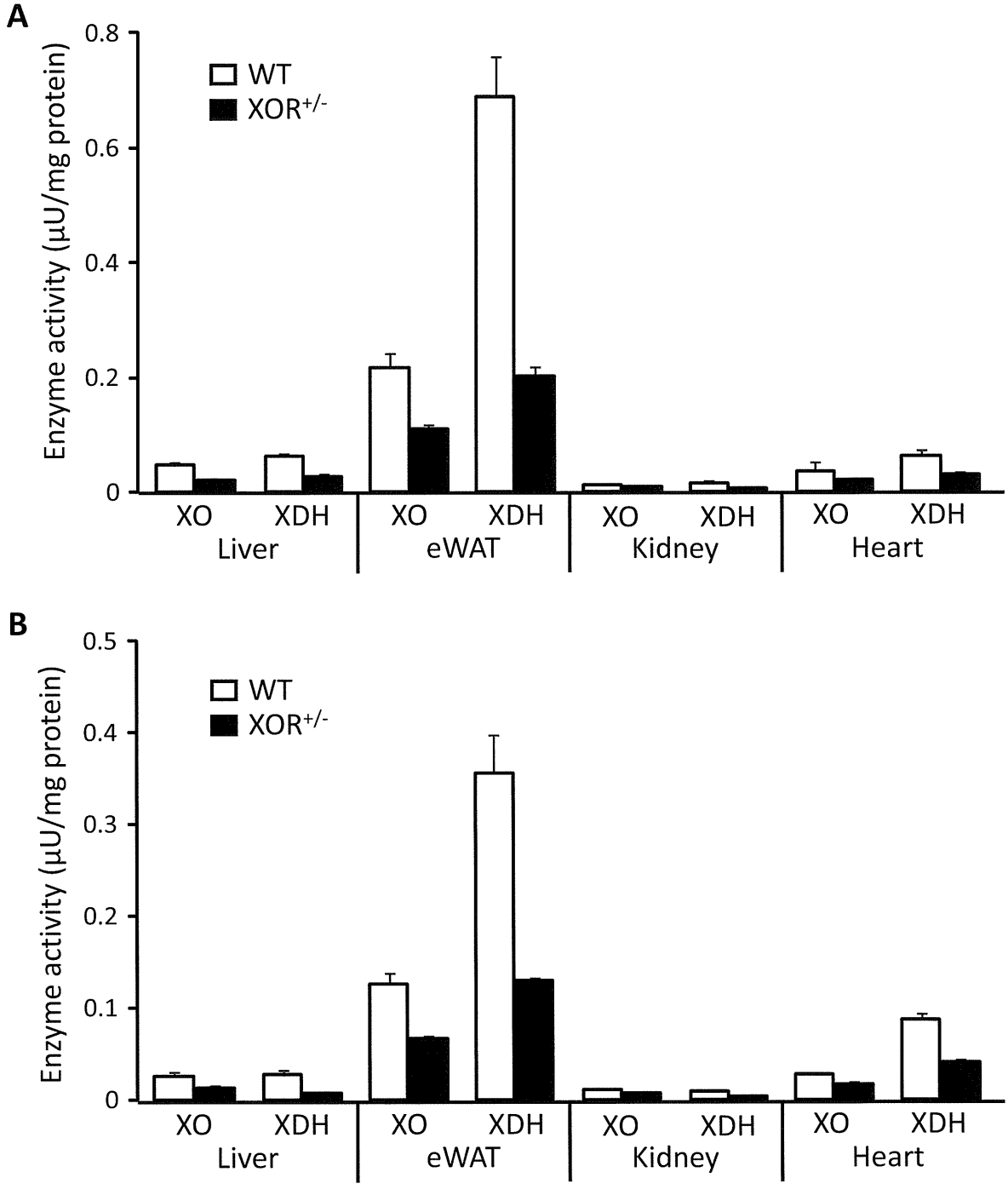

Supplemental Figure II. XOR activity at 2 months (A) and 12 months (B) of age. XOR (XO and XDH) activity of tissue lysates from liver, eWAT, kidney and heart, n=5 per group.

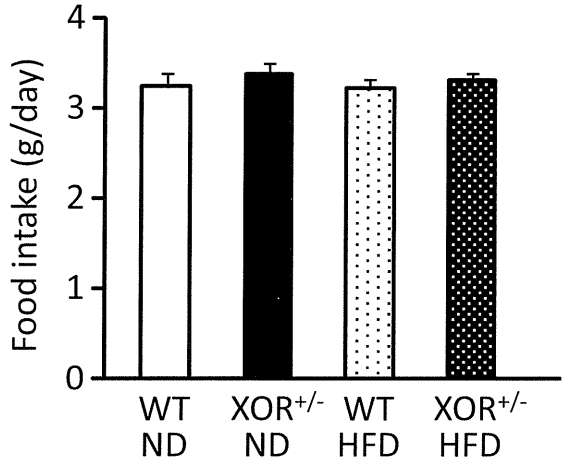

Supplemental Figure III. Amount of daily food intake in four groups with ND or HFD, n=8 mice per group.

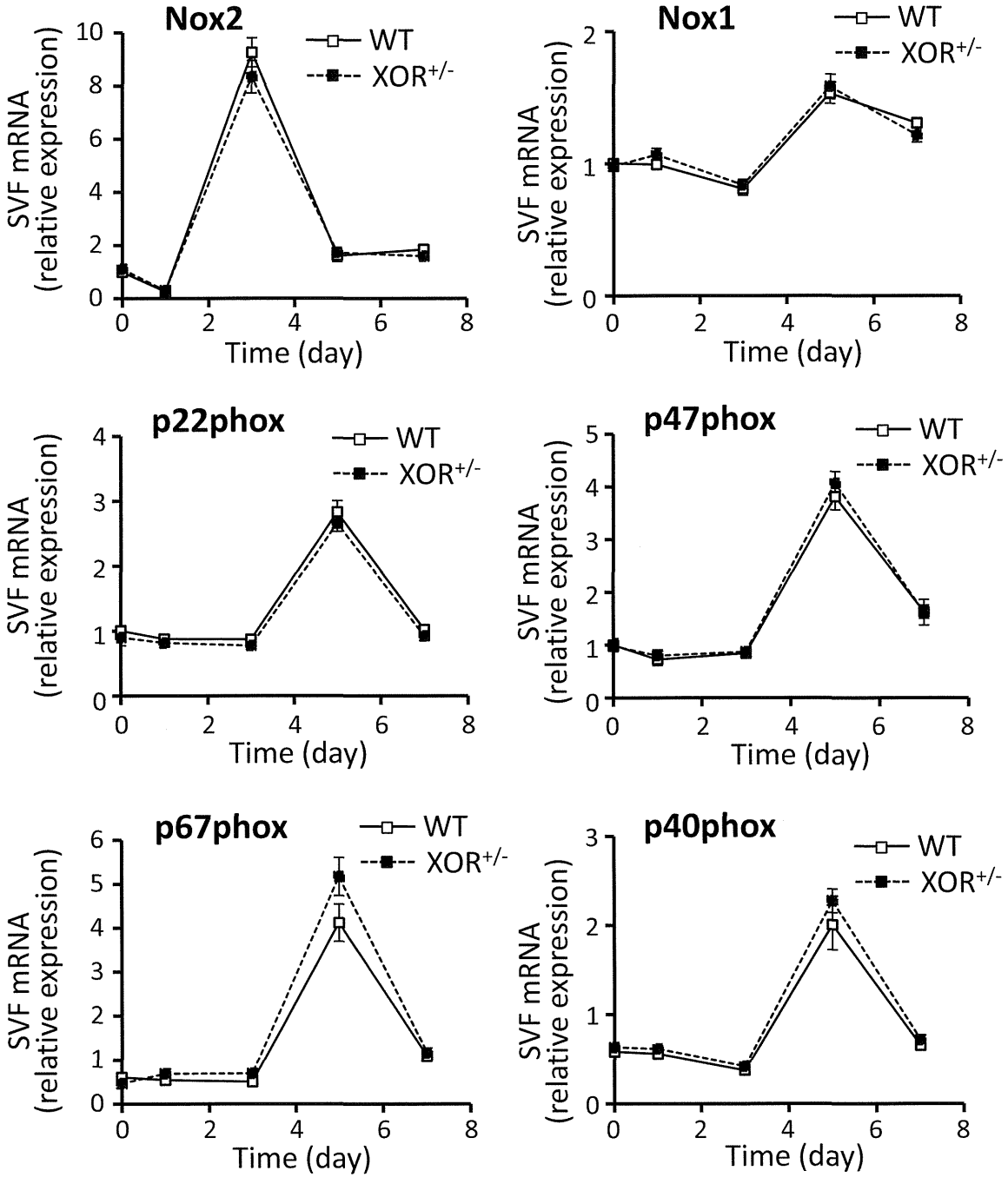

Supplemental Figure IV. Quantitative RT-PCR on SVF cells during post differentiation of WT and $XOR^{+/-}$ mice, n=6 mice per group. Data are normalized by the expression of TBP. Nox indicates NADPH oxidase.

Supplemental Table I. Serum uric acid and lipid variables at 4 and 18 months of age

	WT	XOR+/-	p-value
4months			
Total cholesterol (mg/dl)	81.8 ± 11.8	91.3 ± 10.8	0.56
Free fatty acid (μEq/L)	751.6 ± 85.3	675.8 ± 34.7	0.39
Triglyceride (mg/dl)	20.6 ± 2.8	22.2 ± 2.7	0.69
Phospholipid (mg/dl)	154.1 ± 17.7	158.3 ± 12.1	0.84
18months			
Uric acid (mg/dl)	2.42 ± 0.23	1.18 ± 0.09	0.00001
Total cholesterol (mg/dl)	68.9 ± 3.6	68.4 ± 2.6	0.89
Free fatty acid (μEq/L)	654.8 ± 35.4	518.4 ± 39.0	0.02
Triglyceride (mg/dl)	49.6 ± 6.9	43.9 ± 5.6	0.52
Phospholipid (mg/dl)	144.5 ± 6.6	143.7 ± 4.4	0.91

n=8 per group

Supplemental Table II. Sequences of real-time PCR primer pairs

Gene	Forward (5' → 3')	Reverse (5' → 3')
XOR	GGAGATATTGGTGTCCATTGTG	CCTGCTTGAAGGCTGAGAAA
MCP-1	GCCCCACTCACCTGCTGCTACT	GCCCCACTCACCTGCTGCTACT
TNFα	AAGCCTGTAGCCCACGTCGTA	AAGCCTGTAGCCCACGTCGTA
Adiponectin	GTTCTACTGCAACATTCCGG	TACACCTGGAGCCAGACTTG
Leptin	GATGGACCAGACTCTGGCAG	AGAGTGAGGCTTCCAGGACG
PPARγ	TGTCGGTTTCAGAAGTGCCTTG	TTCAGCTGGTCGATATCACTGGAG
C/EBPβ	ACCGGGTTTCGGGACTTGA	GTTGCGTAGTCCCGTGTCCA
FABP4	TGGGAACCTGGAAGCTTGTCTC	GCTGATGATCATGTTGGGCTTG
FSP27	GTGTCCACTTGTGCCGTCTT	CTCGCTTGGTTGTCTTGATT
Nox4	ACTCCTTGGGTCAGCACTGG	GTTCCTGTCCAGTTGTCTTCG
C/EBPα	TGCGCAAGAGCCGAGATAAAG	TCACGGCTCAGCTGTTCCAC
Nox2	CATCCAGTCTCCAAACATGACAG	GCTACAGTGGCAATCACTCCAGTA
Nox1	CGTGAAAAGATGACCCAGATCA	TGGTACGACCAGAGGCATACAG
p22phox	GTCCACCATGGAGCGATGTG	CAATGGCCAAGCAGACGGTC
p47phox	GATGTTCCCCATTGAGGCCG	GTTTCAGGTCATCAGGCCGC
p67phox	CTGGCTGAGGCCATCAGACT	AGGCCACTGCAGAGTGCTTG
p40phox	GCCGCTATCGCCAGTTCTAC	GCAGGCTCAGGAGGTTCTTC

Materials and Methods

Animals

All animal procedures were conducted under protocols approved by the Committee on Ethics of Animal Experimentation of the Faculty of Medicine, Kyushu University. All mice used in the study were males, housed in a facility on a 12-h light / dark cycle with free access to food and water. *XOR* genetically modified mice were prepared as described previously[1] and were the kind gift of Dr. Toren Finkel (NIH/NHLBI).

Intraperitoneal glucose tolerance test

A glucose tolerance test was performed after 12 h of fasting. Glucose (500 mg/kg) was injected intraperitoneally, blood was obtained from the tail, and the glucose level was measured at 0, 30, 60, 90 and 120 min after injection. The trapezoidal rule was used to determine the area under the curve (AUC) of blood glucose concentrations. Homeostasis model assessment of insulin resistance (HOMA-IR) was calculated by using the following formula: HOMA-IR = 26 x fasting insulin level (ng/ml) x fasting glucose level (mg/dl))/405.

Lipid peroxidation

Epididymal white adipose tissue (eWAT) was homogenized in assay buffer (500 μl/50 mg tissue), then centrifuged at 15,000 rpm for 4 min at 4 °C. The supernatant was used for the assay. The levels of lipid peroxidation in eWAT homogenate were measured as a product of malondialdehyde (MDA) using an assay kit for thiobarbituric acid reactive substances (TBARS) (Northwest Life Science Specialties, LLC) according to the manufacturer's instructions. Absorbance was measured using a Spectra Max M5 microplate reader (Molecular Devices, Sunnyvale, CA).

Hydrogen peroxide production in eWAT

Epididymal WAT was dissected out, placed in phosphate buffered saline (PBS), cut into

2-mm square pieces and incubated at 37 °C for 30 min. Hydrogen peroxide (H_2O_2) released from the tissue was detected using an Amplex Red Hydrogen Peroxide Assay Kit (Life Technologies Corp.).

Blood pressure measurement

Systolic blood pressure was measured with the tail-cuff method using a CODA monitor (Kent Scientific) in the unanesthetized state.

Isometric tension recording

Isometric tension was measured in ring segments of the descending thoracic aorta. The thoracic aortas of mice were cut into 2 mm rings and mounted in 5 mL organ chambers filled with modified Krebs solution aerated with 95% O_2 and 5% CO_2 at 36 °C. Two fine stainless-steel wires were placed through the lumen of the ring; one was anchored, and the other was attached to the mechanotransducer (UM-203; Kishimoto). The rings were stretched to 1g of resting tension. After tissue equilibration, a control contraction in response to 77 mmol/L KCl was elicited. Cumulative dose-response curves for relaxation to acetylcholine and sodium nitroprusside were obtained in the rings pre-contracted with phenylephrine (10^{-5} mol/L).

Histological and immunohistological analysis

Epididymal WAT was fixed for 72 h with 10% formaldehyde at 4°C, and then embedded in paraffin. Sections were cut at 4-μm thickness, mounted on glass slides, deparaffinized, rehydrated through a series of ethanol and washed in PBS.[2] For the measurement of adipocyte size, sections were stained with hematoxylin and eosin. Adipocyte sizes (100 adipocytes per sample) were calculated from cross-sectional areas obtained from perimeter tracings using Image J software (Sun Microsystems). For F4/80 staining, the glass slides were treated with 10 μg/ml proteinase K and 4N HCl. After blocking with 5% skim milk for 30 min at room temperature, the sections were incubated in a humidified chamber at 37°C for 1 h with anti-F4/80 antibody (1:500; AbD Serotec #MCA497R). Then the slides

were incubated with biotinylated anti-mouse IgG antibody, reacted with HRP-conjugated streptoavidin and stained with DAB and H_2O_2. After counterstaining with hematoxylin, the slides were dehydrated and permanently mounted. Macrophage infiltration in adipose tissue was quantitated by calculating the ratio of nuclei of macrophage-positive cells to total nuclei in 5 fields of one slide for each of 4 mice in each group.

High-fat diet feeding

WT and $XOR^{+/-}$ mice at 2 months of age were fed either a normal (fat kcal 10%) or high-fat diet (fat kcal 56.7%) for 2 or 10 weeks.

Isolation of the stromal vascular fraction from eWAT

Epididymal WATs collected from WT and $XOR^{+/-}$ mice at 2 months of age were washed, cut into small pieces in PBS and incubated in Dulbecco's Modified Eagle's Medium (DMEM) containing 0.5% collagenase type 1 and 1% bovine serum albumin (Wako Pure Chemicals Industries) at 37 °C for 60 min. Digested cells were passed through a 100-μm nylon mesh (BD Biosciences), followed by centrifugation at 1,500 rpm for 10 min. The SVF cells at the bottom were washed with PBS then centrifuged at 1,200 rpm for 10 min. The SVF pellet was resuspended in 2 ml of DMEM plus 10% FBS, seeded onto 35-mm collagen-coated dishes at a density of 4×10^5 cells/dish or 96-well plates at a density of 3×10^4 cells/well, and cultured at 37 °C under a humidified atmosphere of 95% O_2 + 5% CO_2.

Induction of differentiation into adipocytes

At 24-h after plating in DMEM plus 10% FBS, differentiation was induced by changing the medium to Visceral Adipocyte Culture Medium ver. 2 (Primary Cell Co., Ltd.). This differentiation medium was replaced every two days, and the cells were harvested on day 7 after the induction of differentiation.

Oil Red O staining

Oil Red O staining was performed to visualize the lipid accumulation in differentiating

adipocytes. SVF cells post-induction of adipocyte differentiation were fixed with 4% paraformaldehyde for 15 min, rinsed in PBS, and stained with Oil Red O (0.3% in 60% isopropanol) for 1 h. For quantification of Oil Red O, stained SVF cells seeded onto 96-well plates were dissolved with 99.5% isopropanol and their absorbance was determined at 520 nm using a microplate reader.

ROS production in SVF cells

H_2O_2 released from the SVF cells was detected using an Amplex Red Hydrogen Peroxide Assay Kit (Life Technologies Corp.). Superoxide production was detected by nitroblue tetrazolium (NBT) assay.[3] NBT was reduced by ROS to a dark-blue, insoluble form of NBT called formazan. At 0, 2, 4, 6 and 8 days after induction of adipocyte differentiation, SVF cells seeded onto a 96-well plate were incubated for 90 min in PBS containing 0.2% NBT. Formazan was dissolved in 50% acetic acid, and its absorbance was determined at 560 nm using a microplate reader. The effects of three inhibitors, apocynin (Sigma-Aldrich #A10809), oxypurinol (Sigma-Aldrich #O6881) and rotenone (Sigma-Aldrich #R8875), on ROS production in SVF cells was examined at day 7 post-differentiation. One hour before the measurement of ROS production by NBT reduction assay, 200 μM apocynin, 100 μM oxypurinol or 100 μM rotenone was added to the culture medium.

Xanthine oxidoreductase activity

XOR activity was measured with a previously described fluorometric assay.[4] The tissues were harvested and homogenized in xanthine dehydrogenase (XDH) assay buffer (50 mmol/L potassium phosphate, pH 7.4, 0.2 mmol/L ethylenediamine-*N,N,N′,N′*-tetraacetic acid, and 1.0 mmol/L phenylmethylsulfonyl fluoride). The homogenates were centrifuged at 15,000 rpm at 4°C for 30 min. Xanthine oxidase (XO) enzyme activity was determined in a total volume of 200 μL consisting of 198 μL of the tissue sample and 2 μL pterin. XDH activity was measured as above but with the addition of 2 μL methylene blue. The

excitation frequency was 345 nm, and the emission wavelength was 390 nm. One unit of activity was defined as 1 μmol isoxanthopterin formed per minute, and XOR activity was determined as the sum of the measured XO and XDH activities.

Quantitative RT-PCR

Total RNAs from eWAT and SVF cells were prepared with an RNeasy Lipid Tissue Mini Kit (QIAGEN). Real-time RT-PCR was performed on an Applied Biosystems 7500 using a One-Step SYBR PrimeScript RT-PCR Kit II (Takara Bio Company) according to the protocol provided by the manufacturer. The sequences of the primers used in real-time PCR are shown in Supplemental Table II.

Statistics

The results are expressed as means ± SEM. The statistical significance of differences between the two groups was determined using Student's *t*-tests. Values of $P < 0.05$ were considered significant.

References

1. Ohtsubo T, Rovira II, Starost MF, Liu C, Finkel T. Xanthine oxidoreductase is an endogenous regulator of cyclooxygenase-2. *Circ Res.* 2004; 95: 1118-1124.
2. Ohtsubo T, Ohya Y, Nakamura Y, Kansui Y, Furuichi M, Matsumura K, Fujii K, Iida M, Nakabeppu Y. Accumulation of 8-oxo-deoxyguanosine in cardiovascular tissues with the development of hypertension. *DNA Repair.* 2007; 6: 760-769.
3. Oliveira HR, Verlengia R, Carvalho CR, Britto LR, Curi R, Carpinelli AR. Pancreatic beta-cells express phagocyte-like NAD(P)H oxidase. *Diabetes.* 2003; 52: 1457-1463.
4. Beckman JS, Parks DA, Pearson JD, Marshall PA, Freeman BA. A sensitive fluorometric assay for measuring xanthine dehydrogenase and oxidase in tissues. *Free Radic Biol Med.* 1989; 6: 607-615.

Genetic variants associated with warfarin dose in African-American individuals: a genome-wide association study

Minoli A Perera, Larisa H Cavallari*, Nita A Limdi*, Eric R Gamazon, Anvar Konkashbaev, Roxana Daneshjou, Anna Pluzhnikov, Dana C Crawford, Jelai Wang, Nianjun Liu, Nicholas Tatonetti, Stephane Bourgeois, Harumi Takahashi, Yukiko Bradford, Benjamin M Burkley, Robert J Desnick, Jonathan L Halperin, Sherief I Khalifa, Taimour Y Langaee, Steven A Lubitz, Edith A Nutescu, Matthew Oetjens, Mohamed H Shahin, Shitalben R Patel, Hersh Sagreiya, Matthew Tector, Karen E Weck, Mark J Rieder, Stuart A Scott, Alan H B Wu, James K Burmester, Mia Wadelius, Panos Deloukas, Michael J Wagner, Taisei Mushiroda, Michiaki Kubo, Dan M Roden, Nancy J Cox, Russ B Altman, Teri E Klein, Yusuke Nakamura, Julie A Johnson*

Lancet 2013; 382: 790–96
Published Online
June 5, 2013
http://dx.doi.org/10.1016/S0140-6736(13)60681-9
See Comment page 749

*Contributed equally
Section of Genetic Medicine, Department of Medicine, University of Chicago, IL, USA (M A Perera PharmD, E R Gamazon MS, A Konkashbaev MS, A Pluzhnikov PhD, Prof N J Cox PhD); Department of Pharmacy Practice, University of Illinois at Chicago, Chicago, IL, USA (L H Cavallari PharmD, Prof E A Nutescu PharmD, S R Patel MS); Department of Neurology and Department of Epidemiology (N A Limdi PharmD) and Section on Statistical Genetics, Department of Biostatistics (J Wang BS, N Liu PhD), University of Alabama at Birmingham, Birmingham, AL, USA; Department of Bioengineering (R Daneshjou BS, N Tatonetti PhD, H Sagreiya MD, Prof R B Altman MD) and Department of Genetics (T E Klein PhD), Stanford University, Stanford, CA, USA; Center for Human Genetics Research (D C Crawford PhD, Y Bradford MS, M Oetjens BS), and Department of Medicine and Department of Pharmacology (Prof D M Roden MD), Vanderbilt University, Nashville, TN, USA; Wellcome Trust Sanger Institute, Wellcome Trust Genome Campus, Cambridge, UK (S Bourgeois MS, P Deloukas PhD); Department of Biopharmaceutics, Meiji Pharmaceutical University, Tokyo, Japan (Prof H Takahashi PhD); Center for Pharmacogenomics, Department of

Summary

Background *VKORC1* and *CYP2C9* are important contributors to warfarin dose variability, but explain less variability for individuals of African descent than for those of European or Asian descent. We aimed to identify additional variants contributing to warfarin dose requirements in African Americans.

Methods We did a genome-wide association study of discovery and replication cohorts. Samples from African-American adults (aged ≥18 years) who were taking a stable maintenance dose of warfarin were obtained at International Warfarin Pharmacogenetics Consortium (IWPC) sites and the University of Alabama at Birmingham (Birmingham, AL, USA). Patients enrolled at IWPC sites but who were not used for discovery made up the independent replication cohort. All participants were genotyped. We did a stepwise conditional analysis, conditioning first for *VKORC1* –1639G→A, followed by the composite genotype of *CYP2C9*2* and *CYP2C9*3*. We prespecified a genome-wide significance threshold of $p<5\times10^{-8}$ in the discovery cohort and $p<0\cdot0038$ in the replication cohort.

Findings The discovery cohort contained 533 participants and the replication cohort 432 participants. After the prespecified conditioning in the discovery cohort, we identified an association between a novel single nucleotide polymorphism in the *CYP2C* cluster on chromosome 10 (rs12777823) and warfarin dose requirement that reached genome-wide significance ($p=1\cdot51\times10^{-8}$). This association was confirmed in the replication cohort ($p=5\cdot04\times10^{-5}$); analysis of the two cohorts together produced a p value of $4\cdot5\times10^{-12}$. Individuals heterozygous for the rs12777823 A allele need a dose reduction of 6·92 mg/week and those homozygous 9·34 mg/week. Regression analysis showed that the inclusion of rs12777823 significantly improves warfarin dose variability explained by the IWPC dosing algorithm (21% relative improvement).

Interpretation A novel *CYP2C* single nucleotide polymorphism exerts a clinically relevant effect on warfarin dose in African Americans, independent of *CYP2C9*2* and *CYP2C9*3*. Incorporation of this variant into pharmacogenetic dosing algorithms could improve warfarin dose prediction in this population.

Funding National Institutes of Health, American Heart Association, Howard Hughes Medical Institute, Wisconsin Network for Health Research, and the Wellcome Trust.

Introduction

Warfarin is the most widely prescribed oral anticoagulant in the USA, with more than 35 million prescriptions in 2011.[1] Complicated by a narrow therapeutic index, warfarin contributes to 33% of hospital admissions related to adverse drug events in individuals aged at least 65 years from the USA.[2] Rapid and predictable therapeutic anticoagulation is difficult because dose requirements vary substantially between patients, but is crucial for safe and effective treatment.[3,4]

Dose variability is affected by single nucleotide polymorphisms (SNPs) in genes encoding cytochrome P450 2C9 (CYP2C9), which metabolises the S-enantiomer of warfarin (more active than the R-enantiomer), and vitamin K epoxide reductase complex 1 (VKORC1), which is the target enzyme for the drug. Both candidate gene studies and genome-wide association studies (GWAS) have consistently shown that *VKORC1* and *CYP2C9* genotypes explain up to 30% of the total variability in warfarin dose requirements in people of European or Asian origin.[5–12] The International Warfarin Pharmacogenetics Consortium (IWPC) has shown that the *VKORC1* –1639G→A SNP (rs9923231), *CYP2C9*2* (rs1799853), and *CYP2C9*3* (rs1057910) can be used with clinical variables to predict warfarin dose.[13,14]

Unfortunately, these commonly studied genetic variants explain substantially less variability in individuals of African descent than in those of European or Asian origin.[5,13,14] African Americans have been absent in previous warfarin GWAS. Importantly, the genomes of people of African ancestry have decreased linkage disequilibrium and increased diversity.[15] Therefore, we aimed to identify novel variants contributing to warfarin dose requirements in African Americans.